

See discussions, stats, and author profiles for this publication at: <https://www.researchgate.net/publication/37431283>

Oxidation of Nitrite by Peroxynitrous Acid

ARTICLE in THE JOURNAL OF PHYSICAL CHEMISTRY A · MARCH 2003

Impact Factor: 2.69 · DOI: 10.1021/jp0269064 · Source: OAI

CITATIONS

25

READS

20

7 AUTHORS, INCLUDING:



Patrick Maurer

22 PUBLICATIONS 366 CITATIONS

SEE PROFILE



Reinhard Kissner

ETH Zurich

69 PUBLICATIONS 2,117 CITATIONS

SEE PROFILE



Ursula Rothlisberger

École Polytechnique Fédérale de Lausanne

292 PUBLICATIONS 8,515 CITATIONS

SEE PROFILE



Willem H Koppenol

ETH Zurich

223 PUBLICATIONS 13,521 CITATIONS

SEE PROFILE

Oxidation of Nitrite by Peroxynitrous Acid

Patrick Maurer,[†] Chris F. Thomas,[†] Reinhard Kissner,[†] Heinz Rüegger,[†] Oswald Greter,[‡] Ursula Röthlisberger,^{†,§} and Willem H. Koppenol^{*,†}

Laboratorium für Anorganische Chemie and Laboratorium für Organische Chemie, Eidgenössische Technische Hochschule Zürich, ETH Hönggerberg, CH-8093 Zürich, Switzerland

Received: September 4, 2002; In Final Form: December 13, 2002

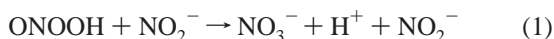
The kinetics of the oxidation of nitrite to nitrate by peroxynitrous acid at pH 5.2 is best described by the rate law $k_{\text{obs}} = k_{\text{iso}} + k'[\text{NO}_2^-] + k''[\text{NO}_2^-]^2$, in which the peroxynitrous acid isomerization rate constant $k_{\text{iso}} = (1.10 \pm 0.05) \text{ s}^{-1}$, $k' = (3.2 \pm 0.1) \text{ M}^{-1} \text{ s}^{-1}$, and $k'' = (4.2 \pm 0.3) \text{ M}^{-2} \text{ s}^{-1}$, at 25 °C. The ternary reaction may involve initial formation of an adduct between nitrite and peroxynitrite, followed by reaction with a second nitrite to form two nitrite and a nitrate. Ab initio calculations indicate that there is only a small intrinsic barrier to the net transfer of HO^+ from peroxynitrous acid to the nitrogen atom of nitrite. A similar transfer to either of the two oxygens of nitrite produces the reactants, and would not lead to an increase in the rate of disappearance of peroxynitrous acid, as observed. The low rate constant is most likely due to stringent orientational constraints. Formal transfer of HO^+ to $^{15}\text{NO}_2^-$ results in formation of $^{15}\text{NO}_3^-$, as experimentally observed. HO^+ transfer is common to the chemistry of peracids, a family of compounds to which peroxynitrous acid belongs.

Introduction

Since the suggestion by Beckman et al.¹ that peroxynitrite might be formed in vivo from the diffusion-controlled reaction of superoxide with nitrogen monoxide,^{2,3} there has been a renewed interest in the chemistry of this unstable isomer of nitric acid.⁴

Peroxynitrous acid is a special peracid in that it not only undergoes a bimolecular disproportionation common to all members of this class of compounds,^{3,5–10} but also isomerizes to nitrate.¹¹ The isomerization is first-order in peroxynitrous acid concentration and may occur via an intramolecular atom shift, or as a rate-limiting homolytic cleavage into a caged radical pair followed by fast recombination of the fragments.¹²

A third pathway to nitrate is possible. It is often neglected that, with the exception of tetramethylammonium peroxynitrite,^{13,14} peroxynitrite preparations are contaminated with nitrite. The nitrite content can be as high as that of peroxynitrite itself. Given a reduction potential for the $\text{ONOOH}/\text{NO}_2^-$, H_2O couple of about 1.6 V at pH 7,¹⁵ and the observation that addition of excess nitrite to peroxynitrous acid affects its decay rate at physiological pH,³ it is possible that some of the nitrate formed during the isomerization could, in fact, arise from the two-electron oxidation of nitrite. In eq 1



the nitrite concentration does not change, and the reaction would normally go unnoticed. Considering that the rate constants for the decay of peroxynitrous acid, obtained with a variety of peroxynitrite preparations with and without major nitrite contamination, all cluster around 1.2 s^{-1} , it can be concluded

that the oxidation of nitrite by peroxynitrous acid, eq 1, is not fast, and, if this reaction were bimolecular, deviations from first-order behavior in the decay of peroxynitrous acid would be observed only at high concentrations of nitrite.

To test whether the reaction in eq 1 occurs during the isomerization of peroxynitrous acid, we investigated the decay of peroxynitrous acid in the presence of [^{15}N]nitrite, which would yield [^{15}N]nitrate. We also studied the kinetics of peroxynitrous acid decay at high concentrations of nitrite.

Experimental Section

Chemicals. $\text{Na}^{15}\text{NO}_2$ was obtained with 99.8% of the nitrite present as [^{15}N]nitrite from Cambridge Isotope Laboratories Inc. (Cambridge, MA). Contamination by nitrate was found to be less than 0.05% by anion exchange chromatography. $\text{Na}^{15}\text{NO}_3$ was prepared by ozonolysis of $\text{Na}^{15}\text{NO}_2$ solutions for 5 min. The completeness of the oxidation was confirmed by anion exchange chromatography. For the synthesis of peroxynitrite,¹⁶ nitrogen monoxide (99.5%) and potassium superoxide (reagent grade) were obtained from Linde (Höllriegelskreuth, Germany) and Aldrich (c/o Fluka, Buchs SG, Switzerland), respectively. Dioxide (99.998%) and argon (99.998%) were purchased from PanGas (Lucerne, Switzerland); all other reagents were purchased from Fluka or Siegfried (Zofingen, Switzerland) in analytical grade quality. Water was purified from deionized water with a Millipore unit.

Peroxynitrite was synthesized from nitrogen monoxide and potassium superoxide as described earlier.¹⁷ Tetramethylammonium peroxynitrite was prepared as described by Bohle et al.¹⁴ Peroxynitrite stock solutions were always freshly prepared and kept on ice and in the dark, and its concentration was determined spectrophotometrically ($\epsilon_{302} = 1700 \text{ M}^{-1} \text{ cm}^{-1}$).¹⁴ The $^{14}\text{NO}_2^-$ impurity in the peroxynitrite was determined by ion chromatography after mixing an aliquot of the cold peroxynitrite solution with 50 mM ice-cooled phosphoric acid and subsequently adjusting to pH ≈ 7 with 50 mM sodium hydroxide. The nitrate concentration was determined chromato-

* Corresponding author. Telephone: 41-1-632-2875. Fax: 41-1-632-1090. E-mail: koppenol@inorg.chem.ethz.ch.

[†] Laboratorium für Anorganische Chemie.

[‡] Laboratorium für Organische Chemie.

[§] Present address: Institute of Molecular and Biological Chemistry, Ecole Polytechnique Fédérale de Lausanne, CH-1015 Lausanne, Switzerland.

graphically and compared to the peroxyxynitrite concentration obtained spectrophotometrically. The difference between these two values was usually about 2% and never exceeded 5%. Nitrogen dioxide was obtained by thermal decomposition of dinitrogen tetroxide prepared by mixing nitrogen monoxide with excess dioxygen at a flow rate of 2 cm³/s in a 50 cm long glass tube, the outlet of which allowed the product gas to be collected in an ice-cooled trap. After collection of 1–2 cm³ of dinitrogen tetroxide, the trap was sealed with a silicone polymer stopper and allowed to warm to room temperature, and the seal was punctured to permit half of the dinitrogen tetroxide/nitrogen dioxide mixture to escape and displace the remaining excess dioxygen before resealing the container.

Methods. ¹⁵N NMR spectra were recorded on a Bruker AMX-500 spectrometer with a field of 11.70 T at 50.49 MHz (Bruker AG, Fällanden, Switzerland). About 10,000 pulses per sample were accumulated overnight. The actual number of pulses was registered for normalization of peak integrals for quantitative analysis. NMR sample tubes were always filled with 0.6 mL of solution. For the quantitative determination of [¹⁵N]-nitrite and [¹⁵N]nitrate, a calibration was carried out by measuring the peak integrals of solutions with known concentrations of pure Na¹⁵NO₂ and Na¹⁵NO₃. Anion chromatography was carried out on a Metrohm 732 ion separation center equipped with a Hamilton PRP X-100 column and a conductometric detector (Metrohm, Herisau, Switzerland), with 2.5 mM phthalate buffer at pH 4.5 as the eluent. UV/vis spectra were recorded on a Kontron Uvikon 820 double beam instrument.

Low concentrations of [¹⁵N]nitrate could not be determined by NMR spectroscopy and, instead, ion chromatography and mass spectroscopy were used to determine the total amount of nitrate and the ¹⁴N/¹⁵N ratio, respectively. Total nitrate was first separated from nitrite and determined quantitatively by ion chromatography. To remove the eluent electrolyte phthalate, which interferes with the mass spectrometric determination, copper metal powder in the presence of sulfuric acid was used to reduce the nitrate to nitrogen monoxide, which was allowed to react in air to form nitrogen dioxide that was collected in neutral water to yield equal amounts of nitrite and nitrate. Ozone was passed through this solution until all nitrite was converted to nitrate. Completion was confirmed by ion chromatography. Since all nitrite was converted to a single species, nitrate, the sensitivity of the mass spectrometric measurements was doubled. For the determination of the ¹⁴N/¹⁵N ratio, samples of the aqueous solution were diluted 1:100 with acetonitrile and introduced through and ionized by an electrospray inlet. Anion mass spectra were recorded on a Finnigan TSQ-7000 mass spectrometer (ThermoFinnigan, MA). The ¹⁵NO₃[−] signal was corrected for the natural abundance of [¹⁵N]nitrogen by means of the ¹⁴NO₃[−] peak in the same spectrum.

Nitrite Oxidation and Isotope Exchange Experiments. Peroxyxynitrite was mixed with 0.25 to 500 mM Na¹⁵NO₂ in alkaline solution at pH = 12; under these conditions, the mixture is stable. The reaction was initiated by rapid mixing via fast simultaneous injection from syringes onto a rotating stir bar in the reaction vessel, 5 mL of the alkaline peroxyxynitrite solution with 5 mL of 0.2 M sodium dihydrogen phosphate in a thermostated flask (25 °C); the pH of the resulting solution was 5.2–5.5, a range in which peroxyxynitrous acid and nitrite anion are the dominant species. After 20 s, the pH was brought to 7 by addition of sodium hydroxide.

The extent of nitrogen exchange between nitrogen dioxide and nitrite was determined as follows: a 100 mL syringe purged with argon was used to remove about 1 mL of the vapor phase

above liquid dinitrogen tetroxide, and the syringe was then filled with argon to enhance dissociation of the gaseous dinitrogen tetroxide present. The average amount of nitrogen dioxide taken into the syringe was determined after repeated injection of its contents into a known volume of rapidly stirred neutral 5 mM phosphate buffer, which was subsequently analyzed for the sum of nitrite and nitrate by ion chromatography. The nitrogen exchange experiment was carried out by injecting the nitrogen dioxide–argon mixture into 100 mM [¹⁵N]-nitrite solutions at pH 5.2, and, after 20 s, the pH was brought to 7 by addition of sodium hydroxide as in the nitrite oxidation experiments.

Kinetics. Solutions of potassium and tetramethylammonium peroxyxynitrite in 5 mM sodium hydroxide were spiked with nitrite to concentrations ranging from 0.1 to 800 mM. These mixtures and a nitrite-free sample were mixed with 0.2 M sodium dihydrogen phosphate in stopped-flow spectrophotometers (SX17MV, Applied Photophysics, Leatherhead, UK, and OLIS RSM-16, Bogart, GA). The pH after mixing was 5.2, which provided extensive hydration of peroxyxynitrite, but not of nitrite. In addition, experiments were carried out at pH 3.6. During these experiments the ionic strength was kept constant at 0.9 M, the difference made up with sodium tetraoxochlorate. The temperature dependence of the rate of isomerization in the presence of 100 and 600 mM nitrite was determined from 15 °C to 50 °C. The disappearance of peroxyxynitrous acid was followed at 265 nm with the Applied Photophysics SX17MV, or by following changes to the spectrum from 250 to 400 nm with the OLIS RSM-16.

Simulations. Kinetics were simulated based on sets of ordinary differential equations with a computer program that implements a two-step implicit Runge–Kutta algorithm of fourth order.¹⁸ This method is more stable than explicit integration techniques, but requires more computation time because of the calculation of the implicit variables. On the other hand, both detection of inherent instabilities and step-width control are easy.

Electronic Structure Calculations. To explore possible mechanisms for a bimolecular reaction of peroxyxynitrous acid and nitrite in the gas phase as well as in aqueous solution, a series of density functional calculations were performed with the ab initio molecular dynamics¹⁹ package CPMD.²⁰ The same computational setup (BLYP functional,^{21,22} soft norm-conserving pseudo potentials,²³ periodic boundary conditions with a basis set of plane waves expanded up to a kinetic energy cutoff of 70 Ry) was used, as in our previous studies on peroxyxynitrous acid.^{24,25} Gas-phase geometries were optimized in an isolated²⁶ simple cubic cell with a box length of 9.0 Å by application of a preconditioned conjugate gradient algorithm. Reaction energy profiles were calculated along different possible reaction coordinates, such as the interatomic distance between the hydroxy oxygen of peroxyxynitrous acid and either the nitrogen atom (“N-attack”) or one of the two oxygens (“O-attack”) of NO₂[−]. Only the *cis*–*cis* conformation of peroxyxynitrous acid, which is predicted by various quantum chemical calculations,^{24,27–29} to be the most stable rotamer in gas phase, has been considered.

The setup of the system in aqueous solution was chosen in analogy to our previous study on the conformational equilibria of peroxyxynitrous acid in water.²⁵ The addition of a single nitrite ion to this system results in a density of 1.005 g/mL, very close to the density of pure water or an aqueous solution of peroxyxynitrous acid and nitrite. The simulation system thus consisted of one ONOOH, one NO₂[−], and 52 H₂O molecules

TABLE 1: Experimental and Calculated Yields (in mM) of [^{15}N]nitrate by the Oxidation of [^{15}N]nitrite with Peroxynitrous Acid at pH 5.2–5.5

initial $^{15}\text{NO}_2^-$ concn	initial HOONO concn	exptl $^{15}\text{NO}_3^-$ yield ^a	yield based on k' and k'' (eq 2)	yield based on homolysis ^b
10	0.5	0.02 ± 0.02	0.01–0.02	0.12
10	1	0.03 ± 0.02	0.03	0.23
10	5	0.21 ± 0.05	0.13–0.15	1.08
10	10	0.24 ± 0.05	0.26–0.30	2.12
100	10	2.5 ± 0.3	2.30–2.60	2.49–2.51
500	10	8.3 ± 0.9	6.83–7.21	3.03–3.06

^a Results are given as $x \pm 2\sigma$, in which x is the average of 6–9 determinations and σ the standard deviation. ^b Based on 40% homolysis, and eqs 7, 11 ($k_{11} = 580 \text{ M}^{-1} \text{ s}^{-1}$), 13a, and 13b. If 30% is assumed, the yields are slightly lower, for instance, 0.12 mM in the fifth column changes to 0.08 mM.

in a periodically repeated simple cubic cell with a box length of 12.0 Å. Hydrogen nuclei were treated as classical particles with the mass of the deuterium isotope. The equations of motion were solved by means of a velocity Verlet integrator with a time step of 7 au (0.169 fs) and a fictitious mass for the electronic degrees of freedom of 1000 au. All simulations were performed at constant volume and a constant temperature of 300 K. During the first ~0.5–1.0 ps of each molecular dynamics run, the temperature of the ions was controlled by velocity rescaling. After this equilibration period, the run was continued with a Nosé–Hoover thermostat³⁰ with a frequency of 500 cm^{-1} coupled to the ionic degrees of freedom. Rough estimates of the relative Helmholtz energies along the reaction coordinate for “N-attack” were performed via thermodynamic integration.³¹ Average values of the constraint force at eight different N–O distances (1.8, 2.1, 2.3, 2.5, 2.8, 3.0, 3.5, and 4.0 Å) were obtained by constrained molecular dynamics runs for each of these states. An additional unconstrained molecular dynamics run was performed to determine the equilibrium N–O distance in the product. The simulation time for each run was between 1.0 and 2.5 ps resulting in a total simulation time of ca. 15 ps for all runs (equilibration not included). The statistical errors of the average constraint force were estimated by calculating the standard deviation of the running averages for windows of 17 fs. These values were also used to estimate the errors of the relative Helmholtz energies.

Results

Product Analysis of the Reaction of HOONO with $^{15}\text{NO}_2^-$

The yield of [^{15}N]nitrate increased steadily with increasing [^{15}N]nitrite concentration: a solution of 500 mM $^{15}\text{NO}_2^-$ and 10 mM HOONO yielded 8.3 mM $^{15}\text{NO}_3^-$. The dependence of the [^{15}N]nitrate yield on initial [^{15}N]nitrite and peroxynitrous acid concentrations is shown in Table 1. The yields for 10, 100, and 500 mM [^{15}N]nitrite with 10 mM peroxynitrous acid were determined by ^{15}N NMR. The results at lower ratios were obtained with mass spectrometry.

Exchange reactions that could add to the yield of [^{15}N]nitrate were experimentally excluded. It was shown by ^{15}N NMR that $^{15}\text{NO}_2^-$ and $^{14}\text{NO}_3^-$ do not exchange within 2 days at pH = 7 and concentrations of 10–100 mM. However, [^{15}N]nitrite slowly produced [^{15}N]nitrate when left at pH = 5.2 for some hours via disproportionation of [^{15}N]nitrous acid. The most critical problem is electron exchange between $^{15}\text{NO}_2^-$ and $^{14}\text{NO}_2^*$. We attempted to measure the extent of this exchange in our reaction system by passing $^{14}\text{NO}_2^*$ diluted with argon into $^{15}\text{NO}_2^-$ solutions, but found no detectable amounts of $^{15}\text{NO}_2^-$. Two rate

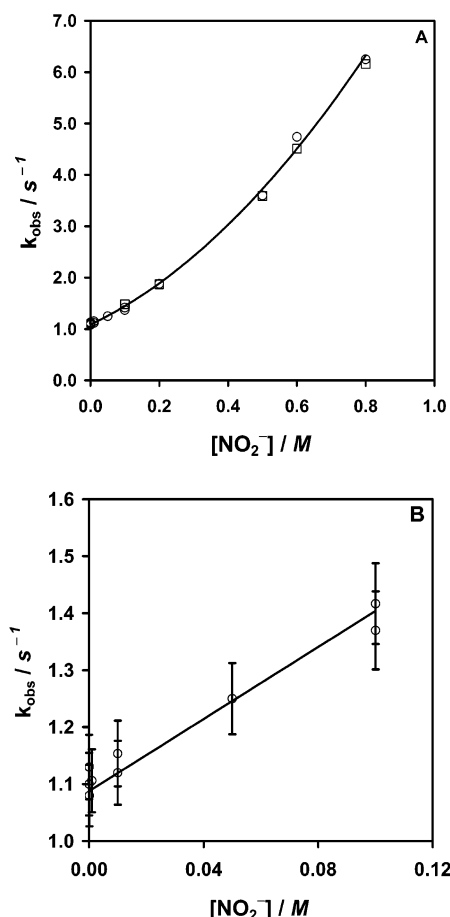


Figure 1. Dependence on the nitrite concentration of the observed rate constant for the combined nitrite oxidation and isomerization of peroxynitrous acid, at 25 °C. (A) all nitrite concentrations, peroxynitrous acid: 0.1 mM. Circles: pH = 5.2, ionic strength of nitrite not constant. Squares: pH = 3.6, sodium tetrachlorate added to nitrite solutions to achieve a constant ionic strength of 0.9 M. (B) nitrite concentrations from 0 to 0.1 M, peroxynitrous acid, 0.1 mM; pH, 5.2. The error bars represent two times the standard deviation. The observation wavelength was 260 nm ($\epsilon_{\text{HOONO}} \approx 600 \text{ M}^{-1}\text{cm}^{-1}$) for all measurements.

constants of this exchange have been published. The first value was estimated from kinetic data of the nitrogen dioxide–nitrite electron exchange reaction by the Marcus cross relationship³² and is $0.02 \text{ M}^{-1} \text{ s}^{-1}$; the second was determined experimentally³³ and is $580 \text{ M}^{-1} \text{ s}^{-1}$. If the small value were correct, the exchange between $^{15}\text{NO}_2^-$ and $^{14}\text{NO}_2^*$ would not be measurable. However, exchange at the higher rate would contribute significantly to the [^{15}N]nitrate yield. Although we found no experimental evidence for this exchange, we did include the rate constant of $580 \text{ M}^{-1} \text{ s}^{-1}$ in the kinetics simulation.

Kinetics. The observed rate constant k_{obs} at pH = 5.2 for the disappearance of 0.1 mM peroxynitrous acid in the presence of nitrite varies from 1.1 – 6.25 s^{-1} at 0–800 mM nitrite, respectively (Figure 1A). The same results were obtained at pH 3.6 and at constant ionic strength (See Supporting Information, Tables 4 and 5, and Figure 1A). Up to 100 mM nitrite, k_{obs} displays an apparent linear dependence on the nitrite concentration (Figure 1B). In the presence of a high excess of nitrite, however, the relation becomes quadratic. The best fit was obtained with eq 2

$$k_{\text{obs}} = k_{\text{iso}} + k'[\text{NO}_2^-] + k''[\text{NO}_2^-]^2 \quad (2)$$

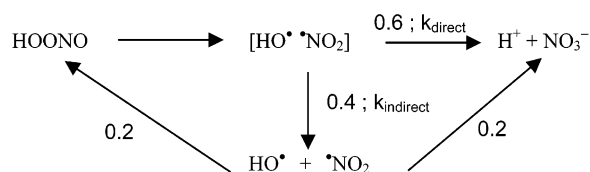
in which the peroxynitrous acid isomerization rate constant k_{iso}

TABLE 2: Reactions Relevant for the Oxidation of Nitrite and [¹⁵N]nitrite by Hydroxyl and Nitrogen Dioxide

reaction		rate constant	reaction no.	ref
HOONO	→ NO ₃ ⁻ + H ⁺	$k_{\text{direct}} = 0.72\text{--}0.9\text{ s}^{-1}$	(5)	see text
HOONO	→ HO• + NO ₂ •	$k_{\text{indirect}} = 0.48\text{--}0.6\text{ s}^{-1}$	(6)	see text
HO• + ¹⁵ NO ₂ ⁻	→ ¹⁵ NO ₂ • + OH ⁻	$k_7 = 1.1 \times 10^{10}\text{ M}^{-1}\text{s}^{-1}$	(7)	a
HO• + NO ₂ ⁻	→ NO ₂ • + OH ⁻	$k_8 = 1.1 \times 10^{10}\text{ M}^{-1}\text{s}^{-1}$	(8)	a
HO• + ¹⁵ NO ₂ •	→ ¹⁵ NO ₃ ⁻ + H ⁺ /HOONO	$k_9 = 1 \times 10^{10}\text{ M}^{-1}\text{s}^{-1}$	(9)	b
HO• + NO ₂ •	→ NO ₃ ⁻ + H ⁺ /HOONO	$k_{10} = 1 \times 10^{10}\text{ M}^{-1}\text{s}^{-1}$	(10)	b
NO ₂ • + ¹⁵ NO ₂ ⁻	→ NO ₂ ⁻ + ¹⁵ NO ₂ •	$k_{11} = 580\text{ M}^{-1}\text{s}^{-1}$	(11)	c
¹⁵ NO ₂ • + NO ₂ ⁻	→ ¹⁵ NO ₂ ⁻ + NO ₂ •	$k_{12} = 580\text{ M}^{-1}\text{s}^{-1}$	(12)	c
2 ¹⁵ NO ₂ • + H ₂ O	→ ¹⁵ NO ₃ ⁻ + ¹⁵ NO ₂ ⁻ + 2 H ⁺	$k_{13} = 6.5 \times 10^7\text{ M}^{-1}\text{s}^{-1}$	(13)	d
2 NO ₂ • + H ₂ O	→ NO ₃ ⁻ + NO ₂ ⁻ + 2 H ⁺	$k_{14} = 6.5 \times 10^7\text{ M}^{-1}\text{s}^{-1}$	(14)	d
NO ₂ • + ¹⁵ NO ₂ • + H ₂ O	→ 1/2 ¹⁵ NO ₃ ⁻ + 1/2 NO ₃ ⁻ + 1/2 ¹⁵ NO ₂ ⁻ + 1/2 NO ₂ ⁻ + 2 H ⁺	$k_{15} = 6.5 \times 10^7\text{ M}^{-1}\text{s}^{-1}$	(15)	d

^a Reference 37. ^b Reference 35. ^c Reference 33. ^d Reference 38, more similar values are found in the Notre Dame Radiation Laboratory database: <http://www.rdc.nd.edu>.

SCHEME 1



$= (1.10 \pm 0.05)\text{ s}^{-1}$, $k' = (3.2 \pm 0.1)\text{ M}^{-1}\text{ s}^{-1}$, and $k'' = (4.2 \pm 0.3)\text{ M}^{-2}\text{ s}^{-1}$, at 25 °C. The rate constant k' was determined in a temperature range from 15 to 50 °C. The activation energy of ca. 50 kJ mol⁻¹ for the bimolecular reaction of peroxyntous acid with nitrite is not very accurate, since the contribution of the isomerization reaction had to be separated; however, it is significantly less than $E_a(k_{\text{iso}}) = (85 \pm 1)\text{ kJ Mol}^{-1}$.³⁴ The rate constant k' is small, not because of the activation energy, but because of the low frequency factor of only about $3 \times 10^9\text{ M}^{-1}\text{ s}^{-1}$. The calculation of the activation energy of the reaction corresponding to k'' is unreliable, since the contributions of the reactions corresponding to k' and k_{iso} have to be factored out. With an already inexact k' , a numerical estimate of $E_a(k'')$ is meaningless. However, it can be said that $E_a(k'')$ is less than or equal to $E_a(k')$. The associated frequency factor is also lower than that associated with k' .

Kinetic Simulations. All kinetic traces obtained could be satisfactorily simulated with the experimentally found expression for k_{obs} , eq 2. The yield of [¹⁵N]nitrate could be simulated with the experimental rate law, eq 2. That is, the k' path yields one [¹⁵N]nitrate for each reaction of [¹⁵N]nitrite with peroxyntous acid, and the k'' path one [¹⁵N]nitrate per two [¹⁵N]nitrites.

A simulation with a model based on up to 40% homolysis of peroxyntous acid into hydroxyl and nitrogen dioxide radicals was also attempted, but did not fit the experimental results (see Discussion). The details of this radical model (Scheme 1) are given in footnote 35. Rate constants for the isomerization and for radical production vary from 0.72 to 0.90 and 0.48–0.6 s⁻¹, respectively.³⁵ All other constants in the reaction scheme were taken from literature, eqs 5–15, and are given in Table 2. For [¹⁵NO₂⁻] \gg [¹⁴NO₂⁻], eqs 8, 10, 12, and 14 can be neglected. For the concentration of the hydroxyl radical, a steady-state condition can be assumed. This can be written as

$$k_{\text{indirect}}[\text{HOONO}] = k_7 \times [\text{HO}^\bullet][^{15}\text{NO}_2^-] \quad (16)$$

since $k_9 \times [^{15}\text{NO}_2^\bullet] \ll k_7 \times [^{15}\text{NO}_2^-]$, which is true because $[^{15}\text{NO}_2^\bullet] \ll [^{15}\text{NO}_2^-]$. Therefore, eq 9 can also be neglected. The yields of ¹⁵NO₂⁻ obtained by computer simulation of the radical model and the empirical rate law are listed in Table 1, for comparison with the experimental results.

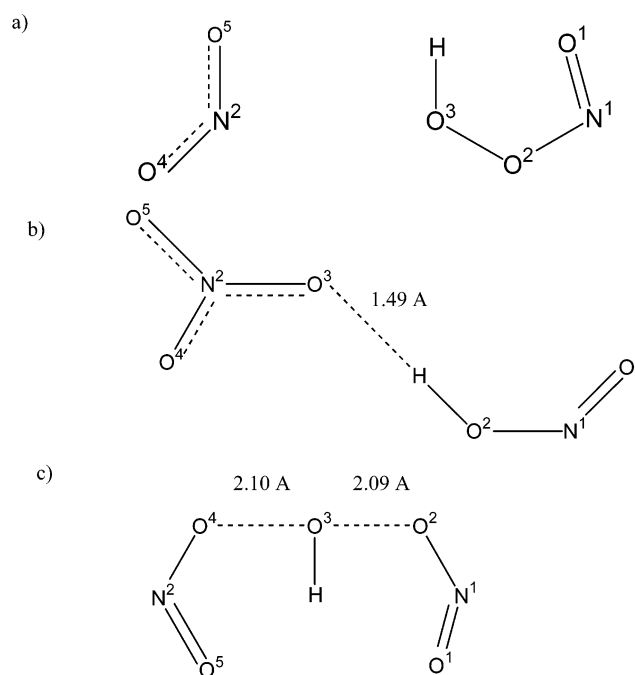


Figure 2. Numbering scheme used in this work and structures of (a) the reactants, (b) the “N-attack” product, and (c) the “O-attack” product. Bond lengths and angles of (b) and (c) are given in Table 1.

Computational Results for the Bimolecular Reaction in Gas Phase. Formally, an S_N2-like reaction with nitrite as both the nucleophile and the leaving group in peroxyntous acid, leads directly to the formation of nitric acid, if the nitrite attacks the oxygen of the hydroxy group of peroxyntous acid with the nitrogen lone pair (“N-attack” pathway). Our calculations show that this reaction can indeed occur barrierless and is exothermic by −173 kJ/mol (Figure 3). The final product is a hydrogen-bonded complex of nitrous acid and nitrate (Figure 2b). Characteristic bond lengths and angles are given in Table 3.

The lone pairs located on the oxygens of nitrite constitute two alternative reactive sites for a nucleophilic attack of nitrite on the substrate peroxyntous acid. We label these two possible pathways “exo” and “endo”, where “endo” denotes an attack of the lone pair closer to O⁵ (Figure 2). For the “exo” pathway, no stable adduct or product structures could be localized whereas the “endo O-attack” occurs again spontaneously and leads to a weakly bound, planar, and almost symmetric adduct (Figure 2c and Table 3), stabilized by 15 kJ/mol with respect to the isolated reactants.

A possible explanation for the absence of any barrier in either the “N-attack” or the “O-attack” case is the very small electronic

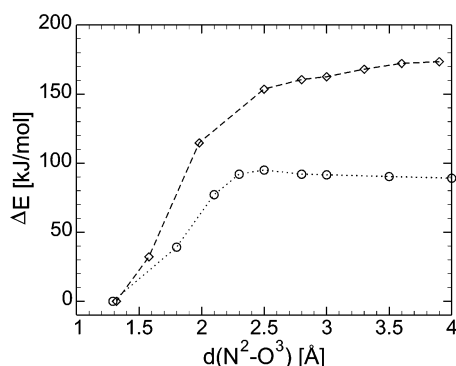


Figure 3. Reaction profiles for the “N-attack” pathway in gas phase (diamonds) and in aqueous solution (circles). Energies are given relative to the two product states.

TABLE 3: Bond Lengths and Angles of the Two Gas Phase Products of the Reaction of Nitrite with Peroxynitrous Acid^a

“N-attack”, Figure 2b		“O-attack”, Figure 2c	
$d(\text{O}^1-\text{N}^1)$	1.23	$d(\text{O}^1-\text{N}^1)$	1.25
$d(\text{N}^1-\text{O}^2)$	1.37	$d(\text{N}^1-\text{O}^2)$	1.26
$d(\text{O}^2-\text{H})$	1.08	$d(\text{O}^2-\text{O}^3)$	2.09
$d(\text{H}-\text{O}^3)$	1.49	$d(\text{O}^3-\text{H})$	0.98
$d(\text{O}^3-\text{N}^2)$	1.32	$d(\text{O}^3-\text{O}^4)$	2.10
$d(\text{N}^2-\text{O}^4)$	1.27	$d(\text{O}^4-\text{N}^2)$	1.26
$d(\text{N}^2-\text{O}^5)$	1.26	$d(\text{N}^2-\text{O}^5)$	1.25
$\angle(\text{O}^1-\text{N}^1-\text{O}^2)$	115.5	$\angle(\text{O}^1-\text{N}^1-\text{O}^2)$	121.5
$\angle(\text{N}^1-\text{O}^2-\text{H})$	112.0	$\angle(\text{N}^1-\text{O}^2-\text{O}^3)$	120.7
$\angle(\text{O}^2-\text{H}-\text{O}^3)$	177.1	$\angle(\text{O}^2-\text{O}^3-\text{H})$	94.3
$\angle(\text{H}-\text{O}^3-\text{N}^2)$	112.4	$\angle(\text{H}-\text{O}^3-\text{O}^4)$	93.0
$\angle(\text{O}^3-\text{N}^2-\text{O}^4)$	119.0	$\angle(\text{O}^3-\text{O}^4-\text{N}^2)$	119.8
$\angle(\text{O}^3-\text{N}^2-\text{O}^5)$	118.3	$\angle(\text{O}^4-\text{N}^2-\text{O}^5)$	121.5
$\angle(\text{O}^4-\text{N}^2-\text{O}^5)$	122.6		

^a Bond lengths are in ångströms and angles in degrees. See Figure 2 for the labeling scheme of the atoms.

rearrangement that is required during the reaction. An analysis of the Kohn–Sham orbitals of the species ONOOH , HNO_3 and NO_2^- reveals that all one-electron orbitals of NO_2^- can be found almost unchanged in ONOOH and HNO_3 . The only exceptions are one of the lone pairs of one of the nitrite oxygens, which is not found in peroxynitrous acid, and the lone pair of the nitrite nitrogen, which is not found in nitric acid. These orbitals are involved in forming the new σ -bond to the hydroxy group, which is not present in nitrite. Formally, both peroxynitrous acid and nitric acid might be considered as nitrite anions with an OH^+ group attached to one of the lone pairs.

Computational Results for the Bimolecular Reaction in Aqueous Solution. Since solvent effects can crucially influence the course and the energetics of a reaction, especially when ionic species are involved, possible bimolecular reaction pathways were also investigated in explicit aqueous solution. Several simulations were performed to gain insight into the effects of solvent and to estimate relative Helmholtz energies along the reaction path. In principle, accurate calculations of relative free energies require extended simulation times, in which all relevant parts of the phase space can be sampled in a statistically significant way. Due to the relatively large computational cost of ab initio molecular dynamics simulations, affordable sampling times are rather limited. However, the mean constraint forces sampled at each point of the reaction coordinate are reasonably well converged and should allow for a first semiquantitative estimation of the relative Helmholtz energies in aqueous solution.

In the gas phase, the “O-attack” case yields a product that is only weakly stabilized (by 15 kJ/mol) and thus can easily decay back to the reactants. The case of the “N-attack” is therefore

the more relevant pathway and only this case was considered for the simulations in aqueous solution. In analogy to the gas-phase results, this reaction yields a hydrogen-bonded complex of nitrous acid and nitrate, which is stable during the time scale of the unconstrained molecular dynamics run (2.5 ps). Relative Helmholtz energies are calculated with respect to the simulation for which the N^2-O^3 distance is maximal (4.0 Å). Compared to this configuration the product is stabilized by 89 ± 20 kJ/mol and an activation barrier of 6 ± 12 kJ/mol is calculated. The resulting Helmholtz energy profile is shown in Figure 3.

Although one can assume that the difference between relative Helmholtz energies (constant volume) and relative Gibbs energies (constant pressure) is negligible, our calculated values cannot be directly compared to the thermodynamic value of -167 kJ/mol¹⁵ for the isomerization of peroxynitrous to nitric acid, because (i) the product in the simulation is $(\text{NO}_3^-\text{HNO}_2)_{\text{(aq)}}$ as opposed to $\text{NO}_3^-(\text{aq}) + \text{H}^+(\text{aq})$ and (ii) in the initial state the peroxynitrous acid and nitrite are too close to be both independently solvated. It can be expected that a separation of the product complex into nitrous acid and nitrate and complete independent solvation of the two species leads to further stabilization, which would be consistent with predicted stabilization being smaller than the thermodynamic value.

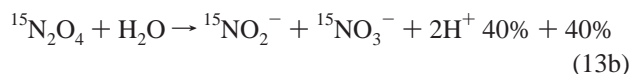
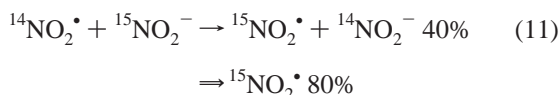
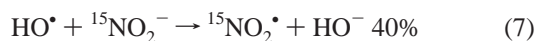
Information about the average structure of the solute and solvent molecules can be obtained from radial distribution functions. Although they are noisy due to relatively short simulation times and limited statistics (there is only one peroxynitrous acid and nitrite molecule present in the simulation box), some structural properties emerge clearly. The results at the maximal separation of the two solutes agree well with the results of a previous study on peroxynitrous acid in water,²⁵ indicating that finite size and concentration effects (the concentration of the two solutes in the simulation is ≈ 1 M each) are relatively small.

The hydrogen bonding pattern of all atoms of the reactant molecules changes quite substantially during the course of the reaction. The radial pair correlation function g_{OHw} of O^1 with the hydrogens of the solvent for instance shows that at the maximal separation of the two solutes and in the product compound, the oxygen atom O^1 is hydrophobic, while at an intermediate N^2-O^3 distance, a hydrogen bond to the solvent can be observed during 90% of the simulation time. This indicates that the solvent cage around the peroxynitrous acid molecule found in the initial stage collapses partially during the course of the reaction and is then built up again around nitrous acid in the product state. These changes in the solvation shells require a substantial rearrangement of the surrounding solvent, in agreement with the possible existence of a small reaction barrier in solution.

Discussion

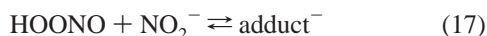
Our results and calculations show that there is a slow, direct reaction between nitrite and peroxynitrous acid that becomes obvious only at higher nitrite concentrations. Given the low rate constant, reactions of peroxynitrite from common preparations are not affected. However, a reaction of nitrite with the reaction product of peroxynitrous acid and an oxidizable substrate may have to be taken into account. One could argue that the nitrite oxidation is mediated by radicals from peroxynitrous acid, as other workers have proposed that peroxynitrous acid should yield up to 40%³⁵ hydroxyl and nitrogen dioxide radicals. If the oxidation were effected by these radicals, and if there were complete exchange between $^{14}\text{NO}_2^\bullet$ and $^{15}\text{NO}_2^\bullet$, then a yield of 40% $^{15}\text{NO}_2^-$ would be predicted; in the absence of such an

exchange, this yield would be 20%.

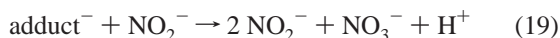


However, the first four entries of Table 1 show that the yields of ${}^{15}\text{NO}_2^-$ are substantially less than 40%, as expected for homolysis plus a fast transfer of the ${}^{15}\text{N}$ -label, and even significantly less than 20%, expected for homolysis alone. Thus, homolysis of the O—O bond is not a viable mechanism. A mechanism consisting of homolysis *and* a direct reaction would predict yields that at low nitrite concentrations differ even more from those determined experimentally.

The observation that the reaction is first-order and, at high concentrations of nitrite second-order, in nitrite supports a mechanism that involves a direct reaction between peroxynitrous acid and nitrite. As ternary reactions are improbable, it is more realistic to assume that the first term (k' , eq 2) is actually composed of an equilibrium followed by a decomposition:



and the third-order process (k'') is invoked under conditions of large excess of nitrite, eq 19.



The structure of the adduct may be similar, but given the small theoretical activation energy not identical, to that shown in Figure 2a, where an attack by N^2 of nitrite on O^3 of peroxynitrous acid would lead to nitrate and nitrite, reaction 18, as discussed above. It is still possible that radical reactions go on in the background, however, they do not contribute significantly, since the radical model [${}^{15}\text{N}$]nitrate yields predicted for low [${}^{15}\text{N}$]nitrite concentrations are much larger than those obtained experimentally (Table 1). When the ${}^{14}\text{NO}_2^\bullet/{}^{15}\text{NO}_2^-$ exchange constant k_{11} of $580 \text{ M}^{-1}\text{s}^{-1}$ is replaced by the older value of $0.02 \text{ M}^{-1}\text{s}^{-1}$, as seems more likely in view of our results, the [${}^{15}\text{N}$]nitrate yields in the simulation of the homolysis model in the presence of 10 mM [${}^{15}\text{N}$]nitrite do not change. Only at higher [${}^{15}\text{N}$]nitrite concentrations is there a contribution from the exchange reaction, no. 11. The experiments at low [${}^{15}\text{N}$]nitrite concentrations suggest that radicals from homolysis of peroxynitrous acid contribute no more than 4–5% to the decay of peroxynitrous acid, most probably less. Inclusion of the direct oxidation of nitrite by peroxynitrous acid in the radical model narrows the difference between experimental and predicted results at higher nitrite concentrations, but worsens it at lower concentrations.

From the results obtained with large excess of nitrite it may be inferred that peroxynitrous acid undergoes a reaction typical for a peracid, namely the apparent transfer of HO^+ .^{8,9} This is another hint that the chemical behavior of peroxynitrous acid is better compared with that of other peracids such as peroxy-

benzoic acid or dihydrogenperoxotrioxosulfate, rather than to that of peroxides. The HO^+ transfer hypothesis is strongly supported by our density functional calculations of the gas-phase reaction of nitrite and peroxynitrous acid. These calculations demonstrate that the direct bimolecular oxidation reaction is a barrier-less process and occurs in $\text{S}_{\text{N}}2$ -like fashion with the lone electron pair of the nitrite nitrogen as the nucleophile and a nitrite anion as the leaving group, which, overall, results in the formal transfer of an HO^+ -moiety from peroxynitrous acid to the attacking nitrite.

A similar picture is obtained from first-principles molecular dynamics simulations in aqueous solution that indicate that there is little or no activation energy needed for the reaction to occur once the two reactants are close enough (ca. 2.5 \AA) and in a proper orientation ($\langle(\text{N}^2-\text{O}^3-\text{O}^2)\rangle$ ca. 120° and the nitrogen lone-pair oriented toward O^3). It should be noted that, at the starting point of the simulation, the two reactants are only 4 \AA apart and already in the correct orientation (a $\langle(\text{N}^2-\text{O}^3-\text{O}^2)\rangle$ angle of ca. 120° and the nitrogen lone-pair oriented toward O^3 turn out to be essential for the reaction to occur). Although the values are different, we conclude that the very low activation barrier of $E_a \approx 6 \text{ kJ/mol}$ in the simulation is consistent with the experimental activation energy of $E_a(k') \approx 50 \text{ kJ/mol}$ and, especially, with the low frequency factor observed experimentally for the following reasons. The maximal N^2-O^3 distance possible in the simulation is 6 \AA , corresponding to half the length of the simulation box. An estimation of the uncertainty in the Helmholtz activation energy if the simulations were extended to this maximal distance yields a value as large as 30 kJ/mol , due to the large statistical error in the average constraint forces. If the reaction rate is determined by desolvation of the reactants and orientational requirements, an accurate determination of the Helmholtz activation energy is far beyond the time scale of ab initio molecular dynamics simulations, because in this case there will be a considerable entropic contribution, an accurate determination of which would require unfeasible simulation times. If, on the other hand, the reaction rate is determined by an enthalpy barrier in the actual chemical reaction of the two reactants, e.g., due to their electronic structure, this barrier would be seen even within the limited time scale of our simulations.

It would seem that the small rate constant observed experimentally is not due to a high activation energy, but rather to the entropic penalty associated with the desolvation of the reacting solutes, and the necessity of bringing them close together in the appropriate orientation for the reaction to occur. This hypothesis is in very good agreement with the experimentally determined low-frequency factor. We can also exclude a formal fast transfer of HO^+ to one of the oxygens of nitrite for two reasons. First, such a reaction would have led to nearly complete [${}^{15}\text{N}$]nitrate formation, which was not observed. Second, since the reactants would have formed back, namely [${}^{15}\text{N}$]peroxynitrous acid and [${}^{14}\text{N}$]nitrite, the rate of decay of peroxynitrous acid would have remained constant and would not have increased as a function of the nitrite concentration.

Peracids undergo bimolecular disproportionation via a formal HO^+ transfer. Earlier we showed that peroxynitrite decay may involve in part disproportionation via a bimolecular mechanism, rather than via homolysis of the O—O bond.^{3,10} The formal transfer of HO^+ to another molecule is shown here.

Acknowledgment. We thank Dr. P. L. Bounds for helpful discussions. Supported by the ETHZ and the SNF.

Supporting Information Available: Tables of observed rate constants of peroxynitrous acid decomposition in presence of

nitrate at variable and at constant ionic strengths. This material is available free of charge via the Internet at <http://pubs.acs.org>.

References and Notes

- Beckman, J. S.; Beckman, T. W.; Chen, J.; Marshall, P. A.; Freeman, B. A. *Proc. Natl. Acad. Sci. U.S.A.* **1990**, *87*, 1620–1624.
- Huie, R. E.; Padmaja, S. *Free Radical Res. Commun.* **1993**, *18*, 195–199.
- Kissner, R.; Nauser, T.; Bugnon, P.; Lye, P. G.; Koppenol, W. H. *Chem. Res. Toxicol.* **1997**, *10*, 1285–1292. Nauser, T.; Koppenol, W. H. *J. Phys. Chem. A* **2002**, *106*, 4084–4086.
- Koppenol, W. H. *Redox Rep.* **2001**, *6*, 339–341.
- Goodman, J. F.; Robson, P.; Wilson, E. R. *Trans. Faraday Soc.* **1962**, *58*, 1846–1851.
- Goodman, J. F.; Robson, P. *Trans. Faraday Soc.* **1963**, *59*, 2871–2875.
- Koubek, E.; Haggett, M. L.; Bataglia, C. J.; Ibne-Rasa, K. M.; Pyun, H. Y.; Edwards, J. O. *J. Am. Chem. Soc.* **1963**, *85*, 2263–2268.
- Koubek, E.; Levey, G.; Edwards, J. O. *Inorg. Chem.* **1964**, *3*, 1331–1332.
- Evans, D. F.; Upton, M. W. *J. Chem. Soc., Dalton Trans.* **1985**, 1153.
- Kissner, R.; Koppenol, W. H. *J. Am. Chem. Soc.* **2002**, *124*, 234–239.
- Anbar, M.; Taube, H. *J. Am. Chem. Soc.* **1954**, *76*, 6243–6247.
- Koppenol, W. H. In *Interrelations Between Free Radicals and Metal Ions in Life Processes*; Sigel, A., Sigel, H., Eds.; Marcel Dekker: New York, 1999; pp 597–619.
- Bohle, D. S.; Hansert, B.; Paulson, S. C.; Smith, B. D. *J. Am. Chem. Soc.* **1994**, *116*, 7423–7424.
- Bohle, D. S.; Glassbrenner, P. A.; Hansert, B. *Methods Enzymol.* **1996**, *269*, 302–311.
- Koppenol, W. H.; Kissner, R. *Chem. Res. Toxicol.* **1998**, *11*, 87–90.
- Systematic names: $\text{O}_2^{\bullet-}$, dioxide(\bullet 1-); NO^\bullet , oxidonitrogen(\bullet); NO_2^\bullet , dioxonitrate(1-); NO_3^\bullet , trioxonitrate(1-); ONOO^\bullet , oxoperoxonitrate(1-). The trivial names superoxide, nitrogen monoxide, nitrite, nitrate and peroxyxynitrite, respectively, are allowed. Leigh, G. J., Ed. *Nomenclature of Inorganic Chemistry*; Blackwell Scientific Publications: Oxford, 1990. Koppenol, W. H. *Pure Appl. Chem.* **2000**, *72*, 437–446.
- Koppenol, W. H.; Kissner, R.; Beckman, J. S. *Methods Enzymol.* **1996**, *269*, 296–302.
- Schwarz, H. R. *Numerische Mathematik*; B. G. Teubner: Stuttgart, 1988; pp 381–383 and 401–406.
- Car, R.; Parrinello, M. *Phys. Rev. Lett.* **1985**, *55*, 2471–2474.
- Hutter, J.; Ballone, P.; Bernasconi, M.; Focher, P.; Foiss, E.; Goedecker, S.; Parrinello, M.; Tuckerman, M. *CPMD*; Max-Planck Institut für Festkörperforschung: Stuttgart, and IBM Research Laboratory: Zürich, 1998.
- Becke, A. D. *Phys. Rev. A* **1988**, *38*, 3098–3100.
- Lee, C.; Yang, W.; Parr, R. G. *Phys. Rev. B* **1988**, *37*, 785–789.
- Trouiller, N.; Martins, J. L. *Phys. Rev. B* **1991**, *43*, 1993–2006.
- Doclo, K.; Röthlisberger, U. *Chem. Phys. Lett.* **1998**, *297*, 205–210.
- Doclo, K.; Röthlisberger, U. *J. Phys. Chem. A* **2000**, *104*, 6464–6469.
- Hockney, R. W. In *Methods in Computational Physics. Advances in Research and Applications*; Alder, B., Fernbach, S., Rotenberg, M., Eds.; Academic Press: New York, 1970; pp 136–211.
- McGrath, M. P.; Rowland, F. S. *J. Phys. Chem.* **1994**, *98*, 1061–1067.
- Tsai, H. H.; Hamilton, T. P.; Tsai, J. H. M.; van der Woerd, M.; Harrison, J. G.; Jablonsky, M. J.; Beckman, J. S.; Koppenol, W. H. *J. Phys. Chem.* **1996**, *100*, 15087–15095.
- Houk, K. N.; Condroski, K. R.; Pryor, W. A. *J. Am. Chem. Soc.* **1996**, *118*, 13002–13006.
- Tuckerman, M. E.; Parrinello, M. *J. Chem. Phys.* **1994**, *101*, 1302–1315.
- Sprick, M.; Cicotti, G. *J. Chem. Phys.* **1998**, *109*, 7737–7744.
- Ram, M. S.; Stanbury, D. M. *J. Am. Chem. Soc.* **1984**, *106*, 8136–8142.
- Stanbury, D. M.; deMaine, M. M.; Goodloe, G. J. *Am. Chem. Soc.* **1989**, *111*, 5496–5498.
- Padmaja, S.; Kissner, R.; Bounds, P. L.; Koppenol, W. H. *Helv. Chim. Acta* **1998**, *81*, 1201–1206.
- Since a scavenger for the hydroxyl radical, namely, $^{15}\text{NO}_2^-$, was in large excess over HOONO in most experiments, it can be assumed that the pathways from the free radicals to nitrate and back to peroxyxynitrite can be neglected. The disappearance rate constant for peroxyxynitrous acid at 25 °C is about $k_{\text{disapp}} = 1.1\text{--}1.2\text{ s}^{-1}$, measured with KOONO and $[(\text{CH}_3)_4\text{I}]\text{-OONO}$ samples, and with the assumption that hydroxyl radicals react mainly with nitrite already present and do not recombine with nitrogen dioxide to form peroxyxynitrous acid, it can be said that $k_{\text{direct}} = 0.6k_{\text{disapp}} = 0.72\text{ s}^{-1}$ and $k_{\text{indirect}} = 0.4k_{\text{disapp}} = 0.48\text{ s}^{-1}$. If, on the other hand, we assume that, in the absence of nitrite, recombination between hydroxyl and nitrogen dioxide radicals take place to form peroxyxynitrous acid and nitrate at a 1:1 ratio (Scheme 1), then

$$k_{\text{disapp}} = k_{\text{direct}} + \frac{k_{\text{indirect}}}{2} \text{ and } \frac{k_{\text{indirect}}}{k_{\text{direct}}} = \frac{0.4}{0.6} \quad (3)$$

which yields

$$k_{\text{direct}} = \frac{k_{\text{disapp}}}{1 + \frac{0.4}{2 \times 0.6}} = 0.90\text{ s}^{-1} \quad \text{and} \quad k_{\text{indirect}} = \frac{k_{\text{disapp}}}{\frac{0.6}{0.4} + \frac{1}{2}} = 0.60\text{ s}^{-1} \quad (4)$$

and an overall decay rate constant of 1.5 s^{-1} for peroxyxynitrous acid. Experimental support for formation of both peroxyxynitrous acid and nitrate after recombination of hydroxyl and nitrogen dioxide radicals was given by Merényi, G.; Lind, J.; Goldstein, S.; Czapski, G. *J. Phys. Chem. A* **1999**, *103*, 5685–5691, in contrast to an earlier report, where only peroxyxynitrous acid was reported.³⁶

(36) Grätzel, M.; Henglein, A.; Taniguchi, S. *Ber. Bunsen-Ges. Phys. Chem.* **1970**, *94*, 292–298.

(37) Barker, G. C.; Fowles, P.; Stringer, B. *Trans. Faraday Soc.* **1970**, *66*, 1509–1519.

(38) Grätzel, M.; Henglein, A.; Lilie, J.; Beck, G. *Ber. Bunsen-Ges. Phys. Chem.* **1969**, *73*, 646–653.